Accepted refereed manuscript of:

Price H, Jones T & BeruBe K (2014) Resolution of the mediators of in vitro oxidative reactivity in size-segregated fractions that may be masked in the urban PM10 cocktail, *Science of the Total Environment*, 485-486, pp. 588-595.

DOI: 10.1016/j.scitotenv.2014.03.056

Resolution of the mediators of *in vitro* oxidative reactivity in size-segregated fractions that may be masked in the urban PM_{10} cocktail

Heather D. Price[a*], *Tim P. Jones*[a], *Kelly A. BéruBé*[b]

Full addresses of where the work was performed:

[a]School of Earth and Ocean Science, Cardiff University, Park Place, Cardiff, CF10 3AT, UK

[b]Cardiff School of Biosciences, The Sir Martin Evans Building, Museum Avenue, Cardiff, CF10 3AX, UK

***Corresponding author (present details):**

Name: Heather Price

Address: School of Geography and Environment, University of Southampton, Southampton, UK, SO17 1BJ

Email: h.price@soton.ac.uk

Authors' email addresses:

Dr Heather Price: h.price@soton.ac.uk

Dr Tim Jones: jonestp@cardiff.ac.uk

Dr Kelly BéruBé: berube@cardiff.ac.uk

Highlights

- The oxidative reactivity (OR) of size segregated PM was tested at a traffic site
- Ultrafine and fine PM size fractions caused more DNA damage than coarse PM
- PM exhibited more OR in comparison to manufactured carbon black particles
- Zn (and Fe) were implicated in the generation of reactive oxygen species in PM
- Size, surface area and metals were important particle characteristics for OR

Abstract

PM_{10} (particulate matter 10 microns or less in aerodynamic diameter) has consistently been linked with adverse human health effects, but the physicochemical properties responsible for this effect have not been fully elucidated. The aim of this work was to investigate the potential for carbon black (CB) particles and PM to generate ROS (Reactive Oxygen Species) and to identify the physicochemical properties of the particles responsible for *in vitro* oxidative reactivity (OR). PM_{10} was collected in 11 size fractions at a traffic site in Swansea, UK, using an Electrical Low Pressure Impactor (ELPI). The PM physicochemical properties (including size, morphology, type, and transition metals) were tested. The plasmid scission assay (PSA) was used for OR testing of all particles. The ultrafine and fine PM ($N_{28\text{-}2399}$; 28 – 2399 nm) caused more DNA damage than coarse PM ($N_{2400\text{-}10,000}$), and the increased capacity of the smaller particles to exhibit enhanced (OR) was statistically significant ($p<0.05$). The most bioreactive fraction of PM was $N_{94\text{-}155}$ with a toxic dose (TD_{50}; mass dose capable of generating 50% plasmid DNA damage) of 69 μg/ml. The mean TD_{35} was lower for PM than CB particles, indicating enhanced OR for PM. A difference between CB and PM in this study was the higher transition metal content of PM. Zn was the most abundant transition metal (by weight) in the ultrafine-fine PM fractions, and Fe in the fine-coarse PM. Through this comparison, part of the observed increased PM OR was attributed to Zn (and Fe). In this study PM-derived DNA damage was dependent upon; 1) particle size, 2) surface area, and 2) transition metals. This study supports the view that ROS formation by PM_{10} is related to physicochemistry using evidence with an increased particle size resolution.

Key Words: Oxidative reactivity, DNA damage, ELPI, PM_{10}, plasmid scission assay (PSA)

1 Introduction

Through respiration, the lung is exposed to a variety of xenobiotics. There is now a well established link between air pollution and associated adverse health impacts (e.g. Stone et al., 2007; Chuang et al., 2013), especially for those in susceptible groups e.g. children, the elderly and those with pre-existing conditions e.g. asthma. Of particular current concern is ambient PM_{10}; particulate matter 10 μm and below. These particles are suspended in the atmosphere and can be both naturally, e.g. crustal, volcanic, and biological, and anthropogenically, e.g. traffic and industrially produced (Jones and BéruBé, 2011; Brown et al., 2011). In urban areas PM_{10} is a heterogeneous "cocktail" of particle types, morphologies, chemistries, and sizes, constantly changing in response to factors including meteorological conditions, season, and geographical location (e.g. Gu et al., 2013; Moreno et al., 2013).

The oxidative capacity of inhaled particles is strongly implicated as a cause of PM_{10} mediated harmful health effects (Ayres et al., 2008; Montiel-Dávalos et al., 2010; Mehta et al., 2013). Oxidative stress is initiated when there is imbalance between oxidants and antioxidants, caused either by an increase in oxidants or a decrease in antioxidants (Chuang et al., 2012). It disrupts the normal functioning of cellular macromolecules, such as lipids, proteins and DNA, and has been linked with respiratory and cardiovascular diseases, pancreatitis and cancer (e.g. Stone et al., 2007; Chuang et al., 2013). The Plasmid Scission Assay (PSA) is a well-established technique for assessing the oxidative capacity, i.e. reactive oxygen species (ROS) - generating capabilities of PM (Lingard et al., 2005; Moreno et al., 2004; Miller et al., 2012). The generation of ROS by particles has been proposed to result from Fenton-type reactions (reactions between Fe^{2+} and hydrogen peroxide (H_2O_2), which forms the highly reactive hydroxyl radical; $^{\bullet}OH$) catalysed by transition metals, including Fe, V, Cr, Co, Ni, Cu, Zn and Ti. Alternatively ROS may arise from direct generation on the particle surface,

which is particularly significant for the ultrafine particles due to high surface area to mass ratios (Baulig et al., 2009). It has also been proposed that the organic compounds associated with PM_{10} generate ROS, as well as endotoxins from bacterial sources (Bonner, 2007).

The particle properties which are responsible for ROS generation remain unclear (Scapellato and Lotti, 2007). Particle size/surface area and transition metal content are two properties which have previously been implicated in particle toxicity (Oberdörster et al., 2005; Koshy et al., 2009; Chuang et al., 2013). Developing our understanding of the particle properties responsible for the observed health impacts from PM_{10} is vital for developing more source-specific air quality policy and for PM reduction targeting (Gil et al., 2010). PM from a specific source generally has a set of characteristics associated with it, e.g. non-exhaust traffic particles in PM_{10} are generally coarse with constituent metals including Ba, Cu, Fe, Zn and Cr (Kwak et al., 2013). If we learn that these types of particles are especially harmful to human health for example, air pollution reductions could be targeted to that source, e.g. funds directed towards improvements in tyre/brake manufacturing and trialling of road wetting in the case of non-exhaust traffic.

The aim of this work was to investigate the potential for CB particles and size-segregated PM_{10} to generate ROS. PM_{10} from an urban traffic hotspot was size-segregated using an ELPI and the oxidative capacity of the 11 different size fractions was assessed. The enhanced size-segregation of the PM in this study in comparison to previous studies allowed separation of the complex PM-mixture into parts, thus allowing a clearer understanding of the role of size, surface area and other factors e.g. metal content to be derived. The objective was to resolve the particle constituent(s) responsible for ROS generation that may be masked in the urban PM_{10} cocktail using high resolution size segregation and comparison with CB.

2 Materials and Methods

2.1 Sampling

Particles were collected into 11 size fractions between 28 nm and 10 μm, as previously described (Price et al., 2010). In brief, particles were collected onto aluminium substrates using an Electrical Low Pressure Impactor (ELPI; Dekati, Finland) at a UK Air Quality Management traffic site in the coastal city of Swansea, south Wales, UK. The site is a major thoroughfare for commuting vehicles into the city, and 16,000 vehicles pass the sampling point every day. Local industry, biological, sea salt particles and others also contribute to the "urban cocktail". Sampling took place during a ten month semi-continuous campaign (January – October 2008). Prior to testing using the PSA, particles were stored in a freezer. Particles were removed from substrates using a novel freeze-dry protocol (Price et al., 2010). Due to the particle yields on individual substrates being below the required mass for the *in vitro* assays, samples across the entire sampling period were combined for each size fraction. The particle sizes in this study are dry particle sizes as determined by the ELPI impactor separation. Size classifications are given as N_{x-y} where x is the D50% cut off for the impactor stage and y is the D50% cut off diameter for the stage above. All sizes are given in nm unless otherwise stated.

2.2 Field Emission Scanning Electron Microscopy (FESEM)

FESEM was used for particle imaging following standard procedures (Jones et al., 2006). Aluminium substrates onto which PM had been collected were dissected and adhered to 12.5 mm aluminium stubs using Epoxy resin (Araldite™). Stubs were coated to improve imaging with evaporated gold-palladium (Au-Pd 60: 40), using a Bio-Rad SC500 sputter coater in an inert argon atmosphere, to a thickness of 20 nm. A Veeco FEI Philips XL30 environmental scanning electron microscope with a field emission gun was used for specimen imaging

(accelerating voltage 5 kV – 20 kV, working distance 5 mm-10 mm, 50 x to 200,000 x magnification).

2.3 Energy Dispersive X-ray (EDX)

For EDX, particles adhered to aluminium stubs using epoxy resin (Araldite™) were carbon coated using a K450 sputter coater (Quorum, UK). Each of the eleven size fractions collected at the traffic site were analysed using an INCA EDX (Cambridge Instruments). Two hundred and fifty individual analyses were carried out for each size fraction of PM_{10} as recommended by previous investigations (Tasić et al., 2006) using a grid system (40s, detection limit of 1 weight percent). Due to their homogeneity 100 spectra were analysed for the CB particles.

2.4 High Resolution-Transmission Electron Microscopy (HR-TEM)

To investigate the insoluble particles collected during the measurement campaign, and to supplement the FESEM investigations, sampled particles were visualised using HR-TEM. Particles were suspended in molecular biology (MB) grade water (Sigma-Aldrich, UK; 2 µg PM/1 µl H_2O) and 40 µl of this suspension was pipetted onto the surface of a 200 mesh Au grid with carbon film (Agar Scientific). Samples were imaged using a Philips CM12 HR-TEM at 80 kV accelerating voltage. Images were taken with a SIS MegaView III digital camera.

2.5 Plasmid Scission Assay (PSA)

Cell-free *in vitro* techniques are useful initial indicators for the OR of different substances. The PSA was chosen for use in this study due to the large number of tests required; it allowed comparison of eleven size fractions of PM (n = 5), while providing results which have been generally shown to correlate with other cell-free *in vitro* techniques (Chuang et al., 2011).

The plasmid ΦX174 RF (Promega, London, UK) was used in this study to assess ROS and/or metal-based damage caused to DNA by both CB particles and PM_{10}. The assay uses purified bacterial DNA (without a cell wall or other cellular components) and therefore can be used to investigate the ROS-sensitivity of different samples, rather than replicate conditions *in vivo*. It is an extremely useful comparative technique and has previously been used to investigate the potential for PM_{10} to damage bacterial DNA (Moreno et al., 2004; Lingard et al., 2005; Chuang et al., 2011; Chuang et al., 2012; Reche et al., 2012).

Particles were suspended in MB H_2O at concentrations between 10 µg/ml and 1 mg/ml. The wide dose range simulated environmental exposure to acute exposure conditions for comparison. Increased resolution of the lower dose range (up to 200 µg/ml) was used to investigate the more "biologically-relevant" concentrations, i.e. lower concentrations which the public is more likely to be exposed to. Nineteen microlitres of the suspensions were then incubated with 200 ng ΦX174 RF DNA for 6 hours at room temperature and gently agitated (Vortex Genie 2; Jencons). Replicates (n=5) were used to assess the precision of the assay. A negative control was run with each batch. The negative control consisted of 19 µl MB grade H_2O incubated with the DNA, with damage levels <10% accepted. The enzyme PST-I (Phenol-Sulfotransferase; Promega, London, UK) was used as a positive control, achieving 100% damage during the 6 hour incubation. Following incubation, 3.33 µl loading dye (Promega, London, UK) was added to each sample. Samples were electrophoresed on a gel consisting of 0.6% agarose (for separation of large DNA fragments) and 0.25% ethidium bromide (for visualisation under UV light when intercalated into DNA). The gel was run for 16 hours at 30 V in a 1 x Tris-Borate-EDTA buffer. Gels were imaged (Visionworks® software, Ultraviolet Products Ltd., UK) to produce an image that could be semi-quantified using Genetools® (Syngene® Systems, UK) via densitometric analysis. Damage levels were derived from the proportion of damaged DNA relative to the proportion of undamaged DNA,

and this was given as a percentage damage value. The negative control (MB H_2O) averaged damage percentage was subtracted from all samples. At even the lowest concentration (10 μg/ml), approximately 25% DNA damage was achieved by both CB particles and PM_{10}. This is either due to intrinsic OR, or represents a baseline to the measurement technique. This was not removed for the calculation of TD_{50}s as it has also been identified in other studies (e.g. Reche et al., 2012). In that study, this baseline was not accounted for and therefore for comparison with previous work this was also not accounted for in our calculations.

2.6 Carbon black (CB) particles

CB particles were used for comparison with PM_{10} to help to elucidate the importance of transition metals in the generation of observed OR. Tested particles were two commercially available CBs (CB-1 and CB-2). CB particles were chosen to mimic the carbon particles which predominate in the nano and fine fractions of PM_{10}; single particles, chains and agglomerates of spherical/sub-spherical carbon.

2.7 Data analysis

Microsoft Excel and SPSS (version 21; SPSS Inc., USA) were used for basic statistical analyses and data plotting. Toxic Dose 50% (TD_{50}) values generated from the PSA were calculated for each size fraction by applying a non-linear regression model (R^2 value, >0.84 for each size fraction) as used in previous studies (Chuang et al., 2012). The independent *t*-test (SPSS version 21; SPSS Inc., USA) was used to compare the mean TD_{50}s for size-fractionated PM_{10} in three size fractions; UF (ultrafine, defined here as 28 nm – 262 nm), fine (263 nm – 2399 nm) and coarse (2400 nm – 10,000 nm). The level of significance for all statistical analyses was chosen as $p < 0.05$.

3 Results and discussion

3.1 Carbon black (CB) physicochemistry

CB particles were used in this study for comparison with heterogeneous airborne PM_{10} mixtures. The physicochemistry of the CB particles (Table 1) highlights similarities with sub-fractions of PM_{10}, particularly the ultrafine-fine PM fractions which are dominated by spherical to sub-spherical carbon particles generated by moving and stationary exhausts (Chuang et al., 2011). For both CB-1 and CB-2, the main constituents (by weight %) were carbon and oxygen. Contamination of CB-1 was below 1% (S, Cu, Si) and for CB-2 below 5% (Cu, Fe, Pb, S, Si).

Table 1 Summary of carbon black physicochemistry. Particle size and morphology obtained from FESEM analysis, and contamination percentage from EDX analysis. Contaminant defined as any unexpected element.

Particle	Particle size (nm)	Morphology	Contamination (%)
Carbon black (CB-1)	100 - 250	Sub-spherical	< 1 (S, Cu, Si)
Carbon black (CB-2)	50 - 200	Sub-spherical	< 5 (Cu, Fe, Pb, S, Si)

3.2 PM_{10} physicochemistry

Particles from a number of different sources were identified at the urban traffic site (Figure 1).

Combustion particles were the most abundant particle type collected at the site by number. Individual soot particles were resolved in size fractions below 100 nm (Figures 1a and 1b), while agglomerates and clusters (Figure 1c) were also found in the fine fractions. These were predominantly carbon particles, but due to the combustion formation process, they were often also associated with surface-bound transition metals (Table 2; Donaldson et al., 2003).

Table 2 Transition metal content of size-segregated PM at the traffic site

Size fraction (nm)	Transition metal content (%)	Specific contributors (%)
N_{28-55}	4.7	Zn (3.6%), Fe (1.0%)
N_{56-93}	4.5	Zn (3.2%), Fe (1.1%), Mn (0.2%)
N_{94-155}	15.4	Zn (14.7%), Fe (0.6%)
$N_{156-262}$	23.6	Zn (23.1%), Fe (0.5%)
$N_{263-383}$	14.1	Zn (11.0%), Fe (2.9%), Mn (0.3%)
$N_{384-615}$	23.2	Zn (22.6%), Fe (0.5%)
$N_{616-952}$	9.4	Fe (7.4%), Zn (1.0%), Mn (1.0%)
$N_{953-1609}$	12.3	Fe (10.5%), Mn (1.3%), Zn (0.4%)
$N_{1610-2399}$	13.7	Fe (11.2%), Zn (1.0%), Mn (1.4%)
$N_{2400-4009}$	11.5	Fe (8.0%), Zn (2.6%), Mn (0.7%), Cu (0.1%)
$N_{4010-10,000}$	10.5	Fe (9.2%), Mn (0.5%), Cu (0.3%), Ti (0.2%)

In urban air these are generally the most numerous particles in PM_{10}, especially in the fine and nano-size fractions. Combustion-derived nanoparticles are emitted from sources including mobile and stationary engines, and traffic combustion particles are considered to be the most harmful common particles to human health (Reche et al., 2012). Industrial particles were discovered in the fine and coarse size fractions (Figure 2), and were of respirable size.

Industrial particles have previously been linked with bioreactivity (Brown et al., 2011). The chemical composition of these particles varied but included transition metals identified in the EDX analysis (Table 2). They were distinct from naturally derived or soot particles due to their larger size and often spherical morphologies from high temperature formation processes

and non-carbon chemical signatures. Mineral particles dominated the coarse fractions of PM_{10} and were considered to be fugitive dust. These particles are generally derived from wind-driven erosion of soil components, resuspension of road dust, and/or construction activities. Fugitive dust components would have contributed to the higher levels of Fe, Mg, and Mn in the fine–coarse particles (Table 2). Marine particles were also found in the coarse fractions of PM (Figure 1e). These can be either directly sourced from the sea or resuspended from road salt during the winter months. Biological particles were identified in some samples, and generally resided in the coarse fractions. Biogenic particles included spores (Figure 1d) which have been linked to allergenic reactions (Donaldson et al., 2003).

3.3 Particle oxidative reactivity (OR)

3.3.1 Carbon black (CB) particles

As the mass-based concentration of CB to which the DNA was exposed to increased, the percentage of DNA damaged during the incubation increased (Figure 3). Neither of the CBs were bioreactive enough to generate a TD_{50}; samples unable to generate 50% plasmid DNA damage are considered to be non-bioreactive (Koshy, 2010). The CBs showed very similar changes in OR with increasing concentration; probably related to their nearly identical sizes and compositions. CB-1 had a TD_{35} of 132 μg/ml while CB-2 was not reactive enough to generate a TD_{35}.

3.3.2 PM_{10}

Concentration-response curves were identified for all PM_{10} size fractions (Figure 4) with the associated TD_{20}s, TD_{35}s and TD_{50}s given in Table 3 for comparison with previous studies using the PSA. As the concentration of particles to which the DNA was exposed to increased, the percentage of DNA damaged during the incubation increased. This was identified for all size fractions. The shape of the concentration-response curve was similar for particles below

2400 nm. In the coarse range (>2400 nm) a flattened response was found. This suggests that increasing the concentration higher than 100 μg/ml had a limited effect on the OR for coarse PM.

The most bioreactive fractions of PM in Swansea were dominated by combustion-derived nanoparticles (CDNP) from the street canyon (Figure 1). CDNP were likely to have originated from vehicle exhausts. Soot particles with nano-powder carbon cores have previously been linked with ROS production (Rouse et al., 2008; Chuang et al., 2011). The least bioreactive fractions of PM were dominated by mineral and sea salt particles. Therefore, the differential chemistry of the coarse, fine and nano-fractions in this study (Table 2) may be linked to source-specific ROS profiles.

Table 3 Comparison of TD_s for this study compared to previous studies. TD_x in μg/ml. TSP = Total suspended particulate. WS = Water soluble.

Particle size (nm)	**TD_{20}**	**TD_{35}**	**TD_{50}**	**Study description**	**Reference**	**Proposed biological driver**
$N_{28\text{-}55}$	13	34	93	Street, Wales, UK	This study	Particle size/surface area, Zn, (Fe)
$N_{56\text{-}93}$	11	30	80	Street, Wales, UK	This study	
$N_{94\text{-}155}$	11	27	69	Street, Wales, UK	This study	
$N_{156\text{-}262}$	15	53	192	Street, Wales, UK	This study	
$N_{263\text{-}383}$	11	38	126	Street, Wales, UK	This study	
$N_{384\text{-}615}$	10	34	120	Street, Wales, UK	This study	
$N_{616\text{-}952}$	20	30	116	Street, Wales, UK	This study	
$N_{953\text{-}1609}$	17	49	145	Street, Wales, UK	This study	
$N_{1610\text{-}2399}$	18	54	162	Street, Wales, UK	This study	
$N_{2400\text{-}4009}$	12	91	677	Street, Wales, UK	This study	

$N_{4010-10,000}$	10	79	625	Street, Wales, UK	This study	
$PM_{10-2.5}$			128-147	Barcelona, Spain	Reche et al., 2012	Size, surface area
$PM_{2.5-0.1}$			28-44	Barcelona, Spain		
PM_{10}			37-102	Incense PM; 3 types tested	Chuang et al., 2011	Size, Cu
$PM_{2.5-0.1}$			185	Urban, Cardiff, UK	Koshy et al., 2009	Size
$PM_{10-2.5}$			493	Urban, Cardiff, UK		
$PM_{2.5-0.1}$			28	Urban-landfill, Cardiff, UK		
PM_{10}	53-260			Satellite city, suburban Beijing, China	Zhou and Song, 2009	Size, WS Zn
PM_{10}	28-480			Clean air site, Beijing, China		
$PM_{2.5}$			10-51	Urban Shanghai, China	Senlin et al., 2008	Size/metals
PM_{10}			100	Indoor smoker, Beijing, China	Shao et al., 2007	WS metals (Zn)
PM_{10}			116	Urban, Beijing, China	Shao et al., 2006	WS Zn
TSP			163	1950s black smoke, London, UK	Whittaker et al., 2004	Chemical composition
PM_{10}			85-106	Industrial area, Wales, UK	Moreno et al., 2004	Chemical composition
$PM_{10-2.5}$			13	Urban, Cardiff, UK	Greenwell et al., 2002	Chemical composition
$PM_{2.5}$			20	Urban, Cardiff, UK		

3.3.3. Comparison to previous studies

Calculated TD_{50} values were within the range of previous studies for different particle size fractions collected in locations worldwide (Table 3), including an industrial area in south Wales (Moreno et al., 2004; TD_{50} = 85 - 106 μg/ml), indoor particles from a smoker's home

in Beijing (Shao et al., 2007; TD_{50} = 100 μg/ml), and London 1950s black smoke (Whittaker et al., 2004; TD_{50} = 163 μg/ml). In a study by Koshy et al. (2009), particles collected in Cardiff, south Wales were divided into two size fractions; $PM_{2.5\text{-}0.1}$ and $PM_{10\text{-}2.5}$. Both Cardiff and Swansea can be considered "large" UK cities by population and are located 50 km apart. In the Koshy study (Cardiff) and this study (Swansea), sampling was undertaken centrally to the city. Both sampling sites were located at the edge of busy routes bisecting the cities. By averaging the size fractions, the TD_{50} for fine ($N_{28\text{-}2399}$) particles in Swansea was 123 μg/ml. This is very similar to the TD_{50} identified for Cardiff in the Koshy study for $PM_{2.5\text{-}0.1}$ (185 μg/ml). At both sites traffic particles (particularly exhaust-derived) would have dominated the collected particles in this size fraction, and due to the proximity of the sampling locations (and hence similarities between the two vehicle fleets) this similarity was expected. The increased OR for fine particles in Swansea is probably related to the lower cut off diameter in Swansea (28 nm) than in Cardiff (100 nm). In the coarse size range, the TD_{50} for $PM_{10\text{-}2.5}$ in Cardiff was 493 μg/ml, which was slightly lower than in Swansea (651 μg/ml) for $N_{2400\text{-}10,000}$. For similar sampling settings in two geographically close cities the ROS generation potential of the PM was similar. This comparability suggests that OR could be generalised more widely than a singular sampling site as long as the site types were the same.

The results from Swansea suggested lower oxidative activity for fine and coarse particles in comparison to "mega cities" and southern European cities. Senlin et al. (2008) collected $PM_{2.5}$ in an urban area in Shanghai, China. Calculated TD_{50}s were between 10-51 μg/ml, which was lower than the equivalent size fraction in Swansea (123 μg/ml). At an urban site in Beijing, China, for PM_{10} a TD_{50} of 116 μg/ml was calculated (Shao et al., 2006). Reche et al. (2012) collected PM in two size fractions ($PM_{10\text{-}2.5}$ and $PM_{2.5\text{-}0.1}$) at an urban site in SW Barcelona. The particles were collected 150m away from one of the busiest roads in the city with a traffic flow of 132,000 vehicles day^{-1}. The TD_{50} for $PM_{2.5\text{-}0.1}$ was between 28-44

μg/ml, which was much lower than in Swansea (123 μg/ml for $N_{28\text{-}2399}$). This shows that for a similar size fraction, the Barcelona PM exhibited greater bioreactivity than Swansea PM. The same was true for coarse particles (128 – 147 μg/ml in Barcelona and 651 μg/ml in Swansea). Barcelona is situated between the mountains and the sea and therefore has one of the highest traffic densities in Europe (6100 cars km^{-2} in comparison to the European average of 1000–1500 cars km^{-2}; Reche et al., 2012). This could account for the increased oxidative activity of the Barcelona PM. In addition, vehicle factors such as fuel composition, vehicle age and type are likely to contribute to differences in the bioreactivity between the two cities.

3.4 Effect of particle size

The nano-size fractions were capable of generating the greatest bioreactive response, as shown by the TD_{50} values (Table 3). The $N_{94\text{-}155}$ fraction with a TD_{50} of 69 μg/ml constituted the most bioreactive fraction, but all the sub-100 nm size fractions exhibited TD_{50}s below 100 μg/ml. This supported the results of previous PSA studies with similar size-dependent results (Lingard et al., 2005; Koshy et al., 2009; Brown et al., 2011), but improved the size resolution. The mean TD_{50}s calculated for different size fractions were compared statistically using the independent *t*-test. For the comparison, particle data were divided into UF (ultrafine 28 nm – 262 nm), fine (263 nm – 2399 nm) and coarse (2400 nm – 10,000 nm). The TD_{50}s for UF and fine size ranges were not found to be statistically significantly different (t = -.957, $p>0.05$), however the TD_{50}s for coarse particles (M = 651 μg/ml, SE = 26.0) were found to be higher than UF (M = 108 μg/ml, SE = 28.3) and fine (M = 134 μg/ml, SE = 8.6) particles, and this difference was significant (t = -11.982, $p<0.05$ and t = 26.007, $p<0.05$ respectively). This shows that there was a statistically significant higher oxidative activity capacity for UF and fine particles in comparison to coarse particles. Classically, low toxicity particles (e.g. CB), below 100 nm, have been shown to induce an increased inflammatory response in comparison to their larger counterparts, and as such particle size is now considered to be a

dominant parameter in influencing lung toxicity (Bonner, 2007). In this study, the enhanced size fractionation achieved by using the ELPI has elucidated the variability in TD_{50} values by size, in comparison to the complex non-fractionated mixtures analysed in previous studies. It has shown for the first time the variability in ROS-generating potential between PM segregated with such high resolution.

3.5 Effect of particle surface area

Particle surface area has been proposed as a driving factor for the enhanced OR of nanoparticles compared to larger particles. Ultrafine particles feature a higher surface area to mass ratio, and therefore, increased surface area per μg in contact with cellular macromoles (i.e. DNA) from which to exert their toxic effects. The surface area per microgram of particles was calculated for all size fractions using a combination of averaged mass and number data acquired by the ELPI during the measurements (Figure 5). This was plotted against the TD_{50} for the corresponding size fraction to illustrate the quantitative relationship between particle surface area and the TD_{50} with high size resolution. An increase in particle surface area was associated with a lower TD_{50}, i.e. greater OR, in comparison to the size fractions with lower surface areas per mass (μg) of particles. It should be noted that the ELPI size fractionates particles using the aerodynamic diameter which assumes a spherical particle shape. While some urban air particles are spherical (e.g. exhaust PM), there are numerous other morphologies observed, e.g. cubic sea salt and elongate flaky mineral particles. The surface area determinations calculated in this study are therefore considered minimum values, and in reality are probably much higher. The trend noted relies on the high TD_{50}s of the two most coarse particle fractions and suggests a two-tiered effect for nano/fine and coarse particles as statistically determined previously.

3.6 Effect of particle-bound transition metals

Surface-bound transition metals are considered to be a further source of OR in PM_{10} (e.g. Lingard et al., 2005). Below 200 nm, PM is generally considered to consist of a carbon core with surface metals. A comparison was made between the TD_{35}s of the urban PM between 100 and 400 nm, and CB-1 (Figure 6), which was found to consist of 100-250 nm diameter carbon particles with <1% transition metal content (Table 1). Only CB-1 was compared since CB-2 was not capable of generating either a TD_{50} or TD_{35} using non-linear modelling. The TD_{35} values for the urban PM were up to four times lower than for the CB. In contrast to the <1% transition metal content of the CB particles, the urban PM was comprised of between 14 and 24% transition metals (by weight). At this site Zn and Fe were important metals in the PM; Zn was the dominant transition metal below 615 nm and Fe was the dominant transition metal above 616 nm. The enhanced OR of UF and fine particles in comparison to CB suggests a driving role for Zn in this study, though this could not be proven statistically.

In a previous study, a similar comparison was made, and the greater inflammatory response from fine PM in comparison to CB was attributed to the surface coating of the fine particles (Pozzi et al., 2003). Transition metals are hypothesised to cause oxidative damage by the generation of ROS through Fenton type reactions and act as catalysts for Haber-Weiss reactions (Könczöl et al., 2013). In a previous study in south Wales, UK, lower TD_{50} levels were associated with Fe, Mn, Ni, Molybdenum (Mo), and especially Zn (Moreno et al., 2004). A study in Beijing found a negative relationship between the TD_{20} and Zn levels (Zhou and Song, 2009), and a study in Xuan Wei, China also found a link between high PM Zn levels and low TD_{50}s (Shao et al., 2013). Fe in PM_{10} has also been implicated in mediating oxidative damage by driving a modified Haber-Weiss or Fenton reaction (Mossman et al., 2007), resulting in the generation of the hydroxyl radical ($^{\cdot}OH$). It is also important to note that in addition to particle size/surface area and transition metals, there may also be other

particle properties which drive the oxidative response which were not analysed in this study (e.g. particle charge and organic constituents).

4. Conclusion

The PSA is an early stage assay for testing the OR of particles and can be considered an initial step towards investigating more holistic health effects of inhalation exposure to PM_{10}. In this study, the oxidative potential of PM_{10} was linked with particle size and surface area; particles within the ultrafine and fine fractions were capable of generating higher levels of oxidative activity than coarse particles. Despite similar particle sizes, the CB particles were less bioreactive than PM_{10} (by TD_{35}), suggesting the generation of oxidative stress by surface reactions on the PM_{10}. An investigation of the transition metal content of the PM implicated Zn (and Fe) in the generation of oxidative activity, though this was not proven directly.

This study has added to previous work by using an enhanced particle size resolution; this allowed the most in-depth analysis of the effect of particle size on OR using the PSA that has been completed to date. A comparison between PM and a surrogate particle type, CB, provided a method to test the contribution to OR of the non-size related physicochemical characteristics. Working with 'cocktails' of PM_{10} from different sources has many confounding factors which complicate the identification of the driver of any biological effect. In this study size segregating the particles was a useful step towards disentangling particles from different sources and with different properties. Future work should continue analysing the OR of particles subdivided into as many size fractions as possible, while moving towards more comprehensive assessment systems, e.g. further *in vitro* assays, testing on cell lines and *in vivo* work. In addition, the use of interventions, e.g. chelators could be used to provide information on the specific chemical constituents which caused OR. Developing our understanding of the particle properties responsible for the observed health impacts from

PM_{10} is important as it has the potential to allow the development of source-specific air quality policy and for PM reduction targeting.

Acknowledgements

Financial support for this work was provided by NERC RCUK.

Competing interests

The authors declare that they have no competing interests.

Author's contributions.

HP carried out the fieldwork, chemical analyses, oxidative reactivity assay and wrote the first draft of the manuscript. TJ was involved in the design of the study and helped with fieldwork. KB was involved in the design of the study, oxidative reactivity assays and revisions of the manuscript. All authors read and approved the final manuscript.

References

Ayres JG, Borm P, Cassee FR, Castranova V, Donaldson K, Ghio A, Harrison RM, Hider R, Kelly F, Kooter IM, Marano F, Maynard RL, Mudway I, Nel A, Sioutas C, Smith S, Baeza-Squiban A, Cho A, Duggan S, Froines J: Evaluating the Toxicity of Airborne Particulate Matter and Nanoparticles by Measuring Oxidative Stress Potential—A Workshop Report and Consensus Statement. *Inhal Toxicol* 2008, 20:75-99.

Baulig A, Singh S, Marchand A, Schins RPF, Barouki R, Garlatti M, Marano F, Baeza-Squiban A: Role of Paris PM2.5 components in the pro-inflammatory response induced in airway epithelial cells. *Toxicol* 2009, 261:126-135.

Bonner JC: Lung fibrotic responses to particle exposure. *Toxicol Pathol* 2007, 35:148-153.

Brown P, Jones T, BéruBé K: The internal microstructure and fibrous mineralogy of fly ash from coal-burning power stations. *Environ Pollut* 2011, 159:3324-3333.

Chuang H-C, Jones T, Chen TT, BéruBé KA: Cytotoxic effects of incense particles in relation to oxidative stress, the cell cycle and F-actin assembly. *Toxicol Lett* 2013, 220(3):229-237.

Chuang H-C, Jones T, BéruBé K: Combustion particles emitted during church services: Implications for human respiratory health. *Environ Intern* 2012, 40:137-142.

Chuang H-C, Jones T, Lung SCC, BéruBé K: Soot-driven reactive oxygen species formation from incense burning. *Sci Tot Environ* 2011, 409:4781-4787.

Donaldson K, Stone V, Borm P, Jiminez LA, Gilmour PS, Schins RPF, Knaapen AM, Rahman I, Faux SP, Brown DM, MacNee W: Oxidative stress and calcium signalling in the adverse effects of environmental particles (PM_{10}). *Free Radic Biol Med* 2003, 34:1369-1382.

Gil PR, Oberdörster G, Elder A, Puntes V, Parak WJ: Correlating physic-chemical with toxicological properties of nanoparticles: The present and the future. *ACS Nano* 2010, 4(10):5527-5531.

Greenwell LL, Moreno T, Jones TP, Richards RJ: Particle-induced oxidative damage is ameliorated by pulmonary antioxidants. *Free Radic Biol Med* 2002, 32:898-905.

Gu J, Schnelle-Kreis J, Pitz M, Diemer J, Reller A, Zimmerman R, Soentgen J, Peters A, Cyrys J: Spatial and temporal variability of PM10 sources in Augsburg, Germany. *Atmos Environ* 2013, 71:131-139.Jones T, BéruBé K: The bioreactivity of the sub-10 μm component of volcanic ash: Soufrière Hills volcano, Montserrat. *J Hazard Mater* 2011, 194:128-134.

Jones T, Moreno T, BéruBé K, Richards R: The physicochemical characterisation of microscopic airborne particles in south Wales: a review of the locations and methodologies. *Sci Total Environ* 2006, 360:43-59.

Könczöl M, Weiss A, Stangenberg E, Gminski R, Garcia-Käufer M, Gieré R, Merfort I, Mersch-Sundermann V: Cell-cycle changes and oxidative stress response to magnetite in A549 human lung cells. *Chem Res Toxicol* 2013, 26:693-702.

Koshy L: The physicochemistry and toxicity of landfill leachates and particulate matter. *Ph.D. Thesis*. Cardiff University, Wales, UK; 2010.

Koshy L, Jones T, BéruBé K: Characterization and bioreactivity of respirable airborne particles from a municipal landfill. *Biomarkers* 2009, 14:49-53.

Kwak J, Kim H, Lee J, Lee S: Characterization of non-exhaust coarse and fine particles from on-road driving and laboratory measurements. Sci Total Environ 2013, 458-460: 273-282.

Lingard J, Tomlin AS, Clarke AG, Healey K, Hay AWM, Wild CP, Routledge MN: A study of trace metal concentration of urban airborne particulate matter and its role in free radical activity as measured by plasmid strand break assay. *Atmos Environ* 2005, 39:2377-2384.

Mehta S, Shin H, Burnett R, North T, Cohen AJ: Ambient particulate air pollution and acute lower respiratory infections: a systematic review and implications for estimating the global burden of disease. *Air Qual Atmos Health* 2013, 6:69-83.

Miller MR, Shaw C, Langrish JP: From particles to patients: oxidative stress and the cardiovascular effects of air pollution. *Future Cardiol* 2012, 8(4): 577-602.

Montiel-Dávalos A, Ibarra-Sánchez M, Ventura-Gallegos JL, Alfaro-Moreno E, López-Marure R: Oxidative stress and apoptosis are induced in human endothelial cells exposed to urban particulate matter. *Toxicol In Vitro* 2010, 24(1):135-141.

Moreno T, Merolla L, Gibbons W, Greenwell L, Jones T, Richards R: Variations in the source, metal content and bioreactivity of technogenic aerosols: a case study from Port Talbot, Wales, UK. *Sci Total Environ* 2004, 333:59-73.

Moreno T, Karanasiou A, Amato F, Lucarelli F, Nava S, Calzolai G, Chiari M, Coz E, Artíñano B, Lumbreras J, Borge R, Boldo E, Linares C, Alastuey A, Querol X, Gibbons W: Daily and hourly sourcing of metallic and mineral dust in urban air contaminated by traffic and coal-burning emissions. *Atmos Environ* 2013, 68:33-44.

Mossman BT, Borm P, Castranova V, Costa DL, Donaldson K, Kleeberger SR: Mechanisms of action of inhaled fibers, particles and nanoparticles in lung and cardiovascular diseases. *Part Fibre Toxicol* 2007, 4(4).

Oberdörster G, Oberdörster E, Oberdörster J: Nanotoxicology: An Emerging Discipline Evolving from Studies of Ultrafine Particles. *Environ Health Perspect* 2005, 113(7):823-829.

Pozzi R, DeBerardis B, Paoletti L, Guastadisegni C: Inflammatory mediators induced by coarse ($PM_{2.5-10}$) and fine ($PM_{2.5}$) urban air particles in RAW 264.7 cells. *Toxicol* 2003, 1(183):243-254.

Price HD, Arthur R, Sexton K, Gregory C, Hoogendoorn B, Matthews I, Jones TP, BéruBé K: Airborne particles in Swansea, UK: their collection and characterization. *J Tox Env Health: Part A* 2010, 73(5):355- 367.

Reche C, Moreno T, Amato F, Viana M, van Drooge BL, Chuang H-C: A multidisciplinary approach to characterise exposure risk and toxicological effects of PM10 and PM2.5 samples in urban environments. *Ecotox Environ Safety* 2012, 78:327-335.

Rouse RL, Murphy G, Boudreaux MJ, Paulsen DB, Penn AL: Soot nanoparticles promote biotransformation, oxidative stress, and inflammation in murine lungs. *Am J Respir Cell Mol Biol* 2008, 39:198-207.

Scapellato ML, Lotti M: Short-term effects of particulate matter: an inflammatory mechanism? *Crit Rev Toxicol* 2007, 37:461-487.

Senlin L, Zhenkun Y, Xiaohui C, Minghong W, Guoying S, Jiamo F, Paul D: The relationship between physicochemical characterization and the potential toxicity of fine particulates (PM2.5) in Shanghai atmosphere. *Atmos Environ* 2008, 42:7205–7214.

Shao L, Hu Y, Wang J, Hou C, Yang, Y, Wu M: Particle-induced oxidative damage of indoor PM10 from coal burning homes in the lung cancer area of Xuan Wei, China. *Atmos Environ* 2013, 77:959-967.

Shao L, Li J, Zhao H, Yang S, Li H, Li W, Jones T, Sexton K, BéruBé K: Associations between particle physicochemical characteristics and oxidative capacity: An indoor PM_{10} study in Beijing, China. *Atmos Environ* 2007, 41(26):5316- 5326.

Shao L, Shi Z, Jones TP, Li J, Whittaker AG, BéruBé KA: Bioreactivity of particulate matter in Beijing air: results from plasmid DNA assay. *Sci Total Environ* 2006, 367:261-272.

Stone V, Johnston H, Clift MJD: Air pollution, ultrafine and nanoparticle toxicology: cellular and molecular interactions. IEEE Transactions of Nano Bioscience 2007, 6:1536-1241.

Tasić M, Đuriæ-Stanojeviæ B, Rajšiæ S, Mijiæ Z, Novakoviæ V, Physico-chemical characterization of PM_{10} and $PM_{2.5}$ in the Belgrade urban Area. *Acta Chim Slov* 2006, 53:401-405.

Whittaker A, BéruBé K, Jones T, Maynard R, Richards R: Killer smog of London, 50 years on: particle properties and oxidative capacity. *Sci Total Environ* 2004, 334-335:435-445.

Zhou L, Song XH: Bioreactivity of Beijing Outdoor Ambient Particulates. In: International Conference on Bioinformatics and Biomedical Engineering Beijing: IEEE: 11th – 13th June 2009, Beijing, China.

Figures

Figure 1: Morphology of typical particles identified during sampling at an urban street canyon; a) and b) combustion derived particles, c) agglomerate of combustion derived particles, d) spherical particle with nodular surface and C-signature suggesting a biogenic particle, e) aged NaCl particle, and f) mineral particle.

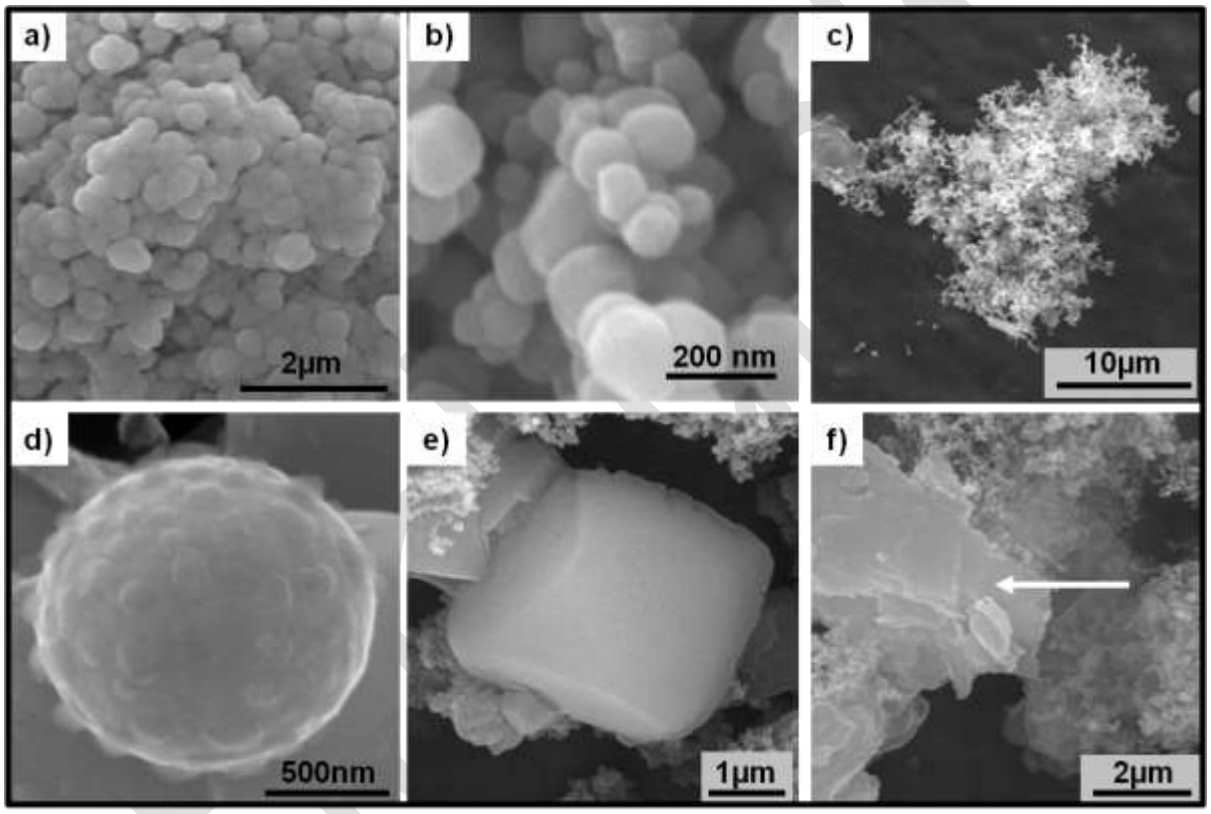

Figure 2: Industrial particles were generally identified in the fine size range; a) aluminium silicate glass particle of 1 μm diameter, and b) spherical carbon-dominated particle of 2.5 μm diameter, both identified using HR-TEM/ EPXMA.

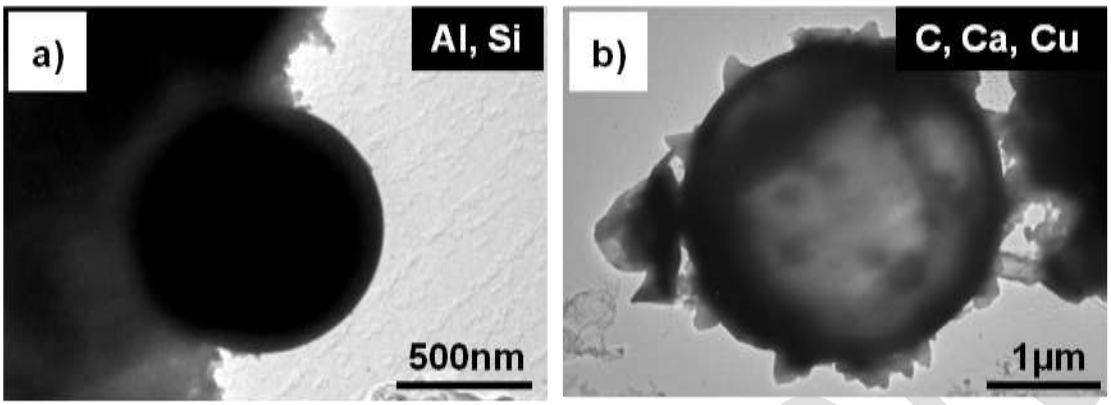

Figure 3: Concentration-response profiles for the carbon black particles; CB-1 and CB-2. Error bars represent 1 SD ± mean, based on n=5.

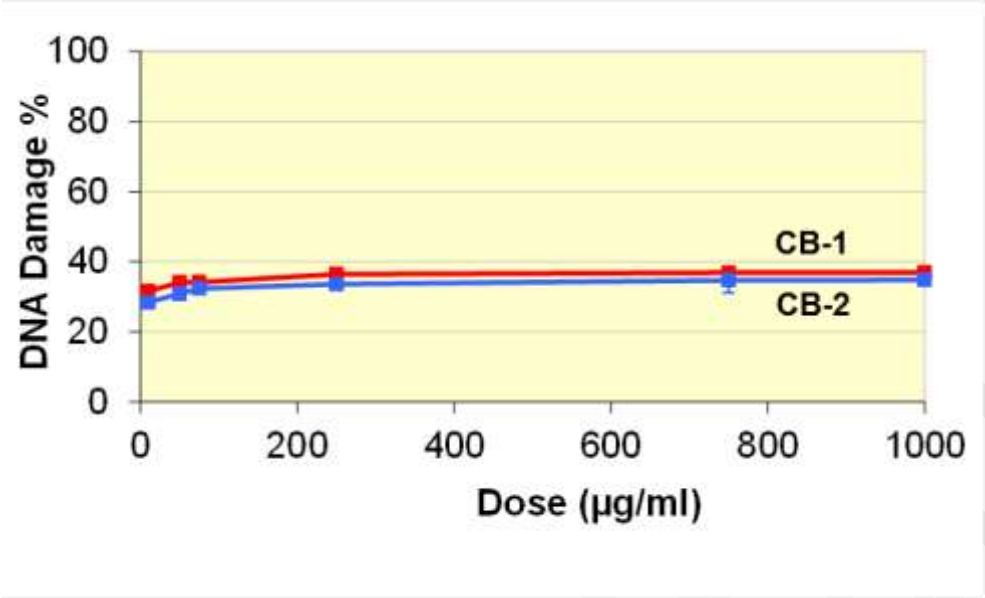

Figure 4: Concentration-response profiles for street canyon PM_{10} ($N_{28\text{-}N10,000}$, a-k). Graphs depict mean ± 1 SD, n = 5. Profiles (a) and (b) represent size fractions below 100nm. Profiles (c) to (i) illustrate results for fine particulate matter. Profiles (j) and (k) are the coarse PM fraction. TD_{50} values were calculated using a non-linear regression model.

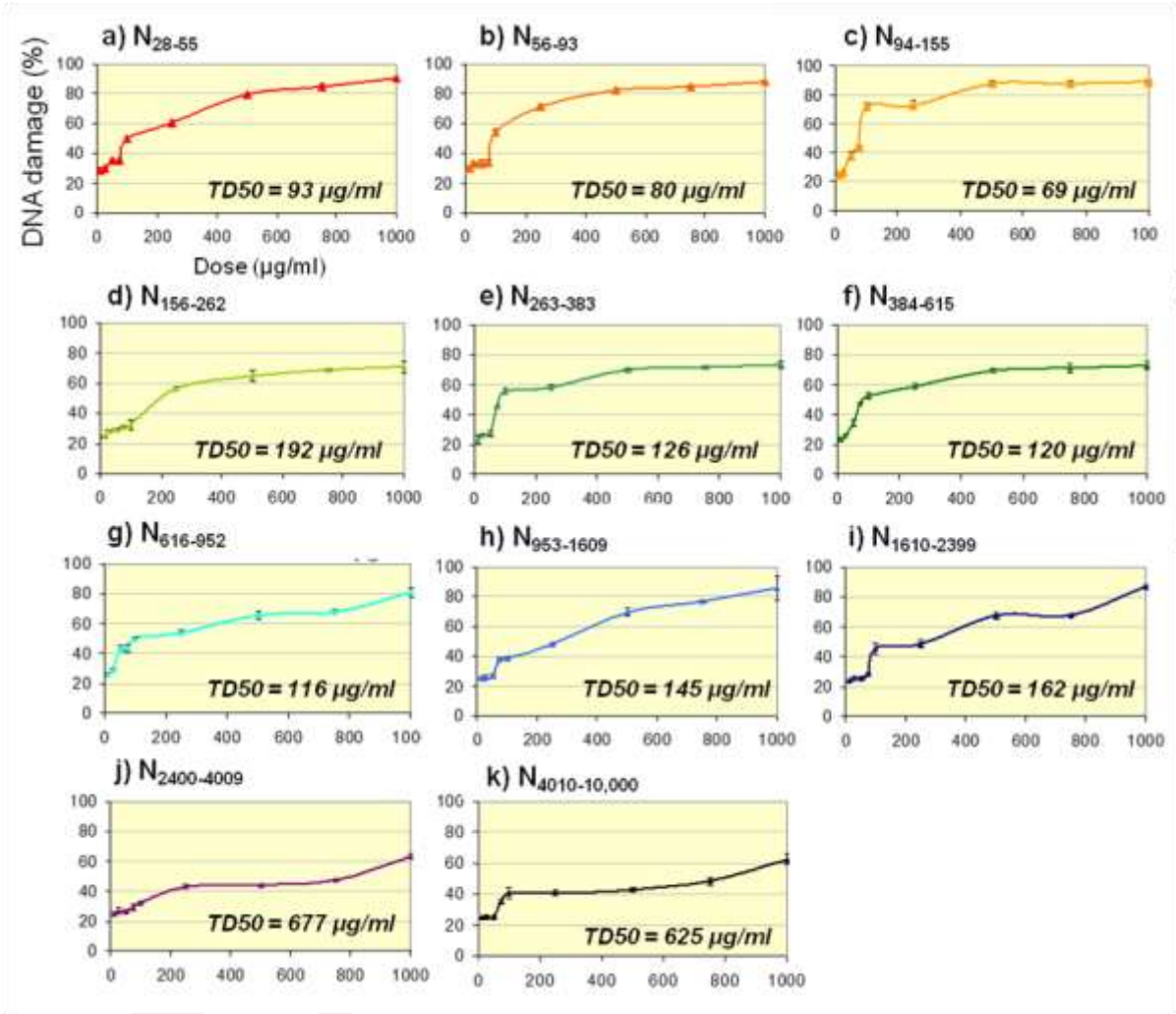

Figure 5: An increase in surface area (SA) is linked with an increase in oxidative reactivity; comparison of TD_{50} and SA for the different PM_{10} fractions; (a) increase in SA with particle size, (b) change in particle mass and particle number in the different particle size fractions. Mass = 1 week average. PNC is depicted by triangles and mass is depicted by squares, (c) scatter plot comparing the calculated SA per microgram of sample with the TD_{50} for each ELPI size fraction.

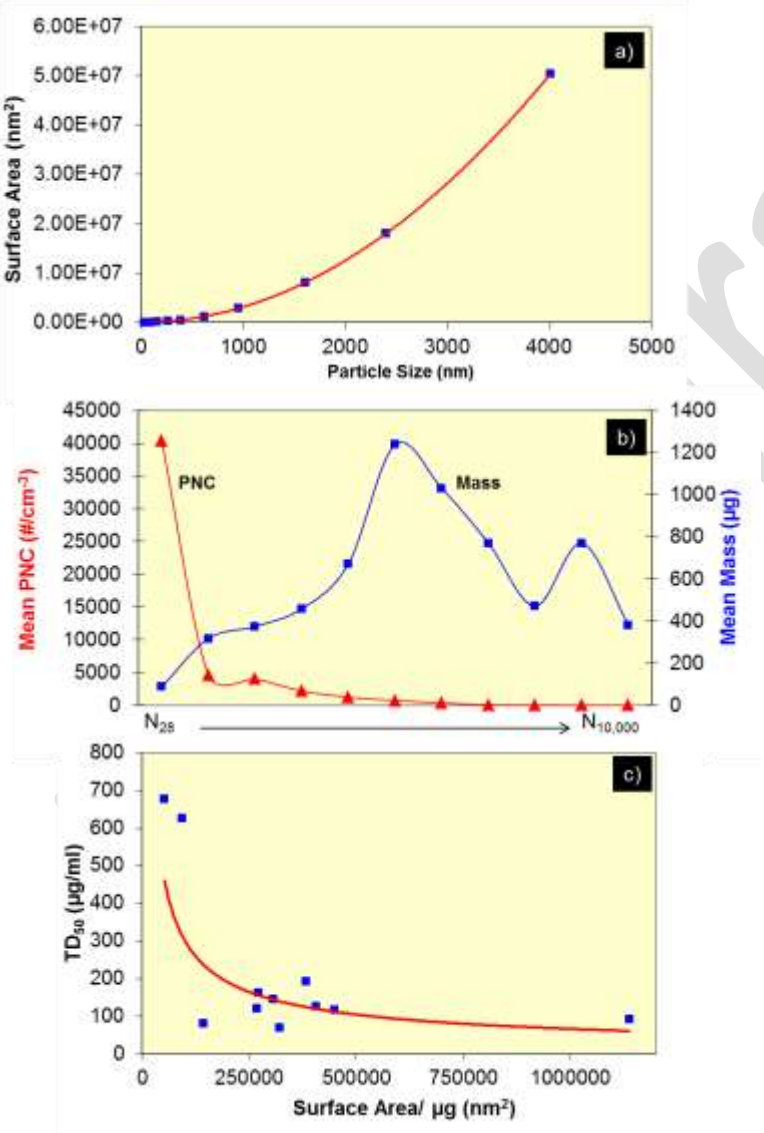

Figure 6: Comparison of carbon black particles (CB-1; 100 - 250 nm) and street canyon particles of an equivalent size; $N_{94\text{-}155}$, $N_{156\text{-}262}$ and $N_{263\text{-}383}$, with their TD_{35} values in µg/ml. Above the graph is shown in diagrammatic form the differential composition of the CB particles and street canyon particles; the CB particles consisted of a carbon core only, whilst the urban air PM was comprised of a carbon core with surface-bound species.